Advanced Powder Technology 24 (2013) 632–642

Contents lists available at SciVerse ScienceDirect

Advanced Powder Technology

journal homepage: www.elsevier.com/locate/apt

Original Research Paper

Towards carbon-free flame spray synthesis of homogeneous oxide nanoparticles from aqueous solutions

Thomas Rudin [1], Karsten Wegner, Sotiris E. Pratsinis *

Particle Technology Laboratory, Institute of Process Engineering, Department of Mechanical and Process Engineering, ETH Zurich, 8092 Zurich, Switzerland

ARTICLE INFO

Article history:
Received 15 August 2012
Received in revised form 18 November 2012
Accepted 26 November 2012
Available online 21 December 2012

Keywords:
Flame aerosol synthesis
Low cost manufacturing
Nitrate precursors
Bi_2O_3, CeO, Al_2O_3 and Cr_2O_3 nanoparticles
Unimodal and bimodal size distributions

ABSTRACT

Flame-assisted spray pyrolysis (FASP) is a versatile process for synthesis of nanoparticles from a broad choice of precursors and solvents. Water is an attractive solvent particularly for inexpensive inorganic precursors (e.g. metal nitrates) as it can effectively reduce the process cost. Furthermore when water usage is combined with a carbon-free fuel (e.g. H_2), nanoparticles can be made without forming CO_2. Here such a FASP process is explored for synthesis of Bi_2O_3 and other oxide nanoparticles from aqueous precursor solutions. The flame temperature was measured by FTIR emission–transmission spectroscopy while powders were characterized by X-ray diffraction and N_2 adsorption. At low FASP fuel gas (H_2 or C_2H_2) flow rates or process temperatures, product powders had a bimodal crystal size distribution. Its large and small modes were made by droplet- and gas-to-particle conversion, respectively. Homogeneous Bi_2O_3 and CeO_2 powders were obtained for sufficiently high flow rates of either C_2H_2 or H_2. Prolonged high temperature residence times promoted precursor evaporation from the spray droplets and yielded homogeneous nanostructured powders by gas-to-particle conversion. In contrast, FASP of aqueous solutions of aluminum nitrate yielded rather large particles by droplet-to-particle conversion at all fuel flows investigated.

1. Introduction

Flame aerosol reactors are widely used for large-scale production of nanostructured commodities such as carbon black, fumed silica, titania, alumina and other ceramics [1]. In recent years, a number of new, sophisticated materials have been developed using flame processes for various applications such as catalysts, biomaterials, nutritional supplements and electroceramics (gas sensors, fuel cells, batteries, etc.) [2,3]. Many are multi-component materials requiring a broad array of compatible precursors [4] that can be quite costly.

Flame processes that involve liquid precursor sprays are employed for the synthesis of these nanomaterials and offer a number of advantages [5], most importantly a proven scalability to kg/h [6,7]. Today, several of such pilot-scale flame spray reactors are operational worldwide [8]. However, for further scale-up to industrial manufacturing level, a reduction of production costs is essential. This could be achieved by employing inorganic metal precursors (e.g. nitrates) dissolved in water that also have a small carbon footprint. Such precursor solutions, however, tend to form inhomogeneous mixtures of nanoparticles by gas-to-particle conversion and much larger, spherical or irregular (e.g. fragmented hollow spheres) particles that are made by droplet-to-particle conversion [9], similar to conventional spray pyrolysis [10,11].

Tani et al. [12] produced ZnO and MgO nanoparticles from combustion of their acetate precursors in methanol/water solutions. The water content in these mixtures should not exceed 40 vol.% for synthesis of homogeneous (unimodal) nanopowders [12]. The same limit of water content in ethanol was found in synthesis of tricalcium phosphate powders by flame-assisted spray pyrolysis (FASP) [13]. More recently, mixed oxide powders were made with FASP [14] using premixed C_2H_2/O_2 as fuel. There, water/dimethylformamide mixtures with up to 75 vol.% water produced homogeneous nanopowders. Using ethanol instead of dimethylformamide resulted in inhomogeneous powders with strong bimodality [14]. When feeding solely aqueous precursor solutions to an oxy/hydrogen flame [15,16], bimodal products were obtained [17,18]. On the other hand, unimodal ZnO, MgO and NiO nanoparticles were made by FASP of aqueous nitrate or acetate precursor solutions [19]. The product particle size distribution changed from bimodal to unimodal by increasing propane flow to the supporting diffusion flame from 2 to 7 L/min. The same was observed for synthesis of mostly unimodal Pb-based-glass powders [20] at up to 4.5 L/min propane and aqueous precursor solution of Pb-nitrate with

* Corresponding author.
E-mail address: sotiris.pratsinis@ptl.mavt.ethz.ch (S.E. Pratsinis).
[1] Current address: Bühler AG, CH-9240 Uzwil, Switzerland.

0921-8831/$ - see front matter © 2012 The Society of Powder Technology Japan. Published by Elsevier B.V. and The Society of Powder Technology Japan. All rights reserved.
http://dx.doi.org/10.1016/j.apt.2012.11.009

tetraethyl orthosilicate. Also, uniform $Ce_{1-x}Gd_xO_{2-x/2}$, nanoparticles were obtained at 7 L/min propane flow in the FASP supporting flame [21].

The above results demonstrate the challenges inherent to production of uniform nanoparticles by spray combustion of aqueous nitrate solutions. Recently a FASP reactor was developed [22] for synthesis of homogeneous oxide nanoparticles from low-cost metal-nitrates (in ethanol) and acetylene or methane as fuel gas. This design was used also for production of unimodal nanostructured iron phosphate [23] for food fortification [24] by direct combustion of C_2H_2 along with the precursor solution spray (Fe-nitrate and tributyl-phosphate in ethanol). This ensured high combustion temperatures facilitating formation of homogeneous products [25].

Here, the focus is on economically attractive, aqueous nitrate solutions as precursors for synthesis of homogeneous nanoparticles by FASP. In addition, the use of H_2 as fuel gas is investigated exploring the potential of a CO_2-free FASP synthesis similar to the commercial oxychloride flame process [26] of simple oxides (SiO_2, TiO_2, etc.). Emphasis is placed in understanding the role of H_2O and H_2 in production of Bi_2O_3 for its electroceramic applications and prior experience in its flame synthesis [22,25,27]. Furthermore, the effect of fuel composition is explored in FASP synthesis of CeO_2, Cr_2O_3 and Al_2O_3.

2. Experimental

2.1. Particle synthesis

Fig. 1 shows the FASP reactor [22] for synthesis of oxide nanoparticles. Fuel (1–12 L/min of C_2H_2, ⩾99.5%, PanGas, or 12–30 L/min of H_2, ⩾99.999%, PanGas) was issued through 12 holes (i.d. 0.5 mm) equidistantly placed at the inner perimeter of a cylindrical torus ring (i.d. 1.6 cm) coaxially to and at 1 cm above the nozzle issuing the precursor solution spray. A stainless steel tube (i.d. 1.6 cm) was placed between ring and nozzle to shield the spray from air entrainment [22]. Precursor solutions were fed through the central nozzle by a syringe pump (Lambda, VIT-FIT) at 2 mL/min and atomized by co-flowing 6 L/min of oxygen (⩾99.5%, PanGas) through the surrounding annulus at 1.5–1.7 bar pressure drop. Additional sheath oxygen was supplied through 32 holes of 0.8 mm diameter each surrounding the nozzle at 1.5 cm radius. All gas flow rates were controlled by calibrated mass flow controllers (Bronkhorst, EL-FLOW). Using a vacuum pump (Busch, Mink MM1202 AV), product particles were collected on water-cooled glass microfiber filters (Albet LabScience GF 6, 25.7 cm in diameter) placed at least 60 cm above the burner.

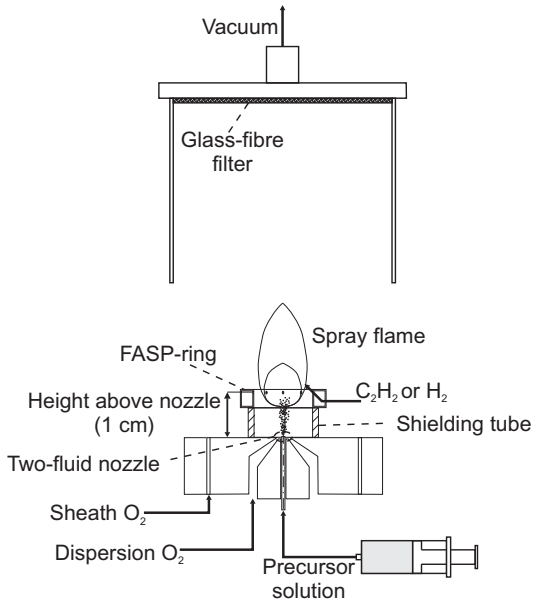

Fig. 1. FASP reactor consisting of a two-fluid nozzle for atomizing the liquid precursor with oxygen and a cylindrical torus (FASP) ring with boreholes to inject and combust C_2H_2 with the precursor solution spray. The ring was located at 1 cm above the nozzle and the spray was shielded from air entrainment by a tube.

Bismuth trinitrate pentahydrate (purity > 98%; Aldrich) was dissolved in 15 vol.% concentrated nitric acid (65% in water, Fluka) and mixtures of deionized ultrapure water (Milli-Q) and denaturized absolute ethanol (A15, Alcosuisse), $y = V[H_2O]/(V[H_2O]+V[EtOH])$, to give a Bi concentration of 0.4 M. In calculating y, the contribution from hydrated water of the nitrate precursor is neglected. Cerium nitrate hexahydrate (99%, Aldrich), aluminum nitrate nonahydrate (⩾98.5%; Fluka) and chromium nitrate nonahydrate (99%, Sigma–Aldrich) were dissolved in pure water to a 0.2 M metal concentration.

2.2. Particle characterization

The specific surface area (SSA) of the powders was determined by N_2 adsorption at 77 K (Tristar, Micromeritics Inc.) and their morphology was obtained by scanning electron microscopy (FEI Quanta 200 FEG) or transmission electron microscopy (FEI Tecnai F30 FEG). The BET equivalent particle diameter was calculated from the SSA assuming spherical primary particles with homogeneous density (ρ_{Bi2O3} = 8.9 g/cm^3; ρ_{CeO2} = 7.2 g/cm^3) [28].

The powder crystallinity was determined by X-ray diffraction (XRD; Bruker D8 Advance, equipped with Lynxeye detector, 40 kV, 40 mA, Cu Kα radiation, Bragg–Brentano geometry) at $15° < 2\theta < 70°$ with a step size of 0.01° for a total measurement time of 5 min. The XRD patterns were analyzed using Topas 4.2 software (Bruker AXS). Phase composition and crystal sizes were obtained by Rietveld refinement [29]. A Chebychev function of up to 15th polynomial order [30,31] was used for background correction. For product powders with bimodal crystal size distribution, the pattern was reconstructed by two superimposed modes using a narrow and a wide Lorentzian with large (200 nm) and small (20 nm) initial sizes [22,27]. Thereby the average crystallite size and mass-fraction for each mode were obtained. To detect the presence of a bimodal crystallite size distribution, the "goodness of fit" (GOF) figure of merit was employed [22,32]. The GOF-value is an index of agreement between calculated and measured XRD patterns here. Smaller GOF-values stand for better fit quality, while for a perfect fit, the GOF should be one [32].

2.3. Flame temperature

Flame temperatures were measured by non-intrusive line-of-sight Fourier transform infrared (FTIR) emission/transmission (E/T) spectroscopy [33,34] (Bomem MB155S) at 8000–500 cm^{-1} with a resolution of 32 cm^{-1} and a beam diameter of 4 mm. Path correction spectra for the emission measurements [35] were taken using a calibrated blackbody cavity (PYROcal® LAB; Transmetra GmbH) in place of the flame. Transmission measurements were averages of 512–1024 scans using an IR bandpass filter (3850–4910 nm; Laser components) in front of the detector allowing to selectively trace the radiation from the hot CO_2 band (≈2100–2400 cm^{-1}). Emission spectra were taken without such a filter, averaging 256–512 scans for each measurement point. The average flame temperature was determined by averaging the temperatures obtained from the Normrad and E/T procedures matching the blackbody Planck function with the hot CO_2 bands from 2300 to 2220 cm^{-1} [34–37]. Error bars represent the deviation of the Normrad and E/T procedures.